spond to the distance from dynamical center, radial velocity, and time rate of change of true anomaly, respectively The first nine and last three data combinations listed correspond to types A and B, respectively

References

[1] Gersten, R H and Schwarzbein Z E, "Self-contained orbit determination techniques," AIAA Preprint 63 431 (August 19–21, 1963)

[2] Schwarzbein Z E and Gersten, R H, "Preliminary orbit determination for a moon satellite," AIAA J 1, 467–469 (1963)

[3] Herrick, S, *Astrodynamics* (D Van Nostrand Company, Inc, Princeton, N J, in Press)

[4] Baker, R M L, Jr and Makemson, M W, *An Introduction to Astrodynamics* (Academic Press Inc, New York, 1960), Chap 6, pp 111–152

[5] Liu, A, Two body orbit determination from two positions and time of flight" Aeronutronic TN 4 (January 2, 1959)

[6] Plummer, H C, *An Introductory Treatise on Dynamical Astronomy* (Dover Publications, Inc, New York, 1960), pp 24–27

Effect of a Cavitating Venturi on Wave Propagation in a Duct

L R Iwanicki* and O W Dykema†
North American Aviation, Inc, Canoga Park, Calif

Introduction

A VENTURI designed to reduce the static pressure of the fluid flowing through the throat to its vapor pressure is termed a cavitating venturi When operating under this condition, assuming a constant upstream head, a decrease in pressure downstream of the venturi will not result in increased flow [1–4]

The purpose of this investigation, conducted for NASA, was to determine whether or not the cavitating venturi is effective in maintaining a constant flow when the downstream pressure oscillates in the frequency range of 100–1000 cps If the answer to this question is affirmative, this characteristic of the cavitating venturi could be useful when applied as a dynamic decoupling device in liquid rocket engines A logical location would be at the discharge end of the feed system to effectively decouple combustion and propellant feed system oscillations

Test System Configuration and Instrumentation

The function of the test system is to simulate the environment and boundary conditions that will exist in the actual application of the venturi To facilitate test programming, water was used as the test medium in conducting initial tests to study the effect of cavitating venturi action in a dynamic flow system Later, liquid oxygen replaced water to confirm that no serious deviations in this characteristic action resulted from a change in the test medium

A sketch of the test system configuration is shown in Fig 1 The system consists essentially of a 1-in -i d pipe, approximately 10 ft long, bounded at the upstream end by a large tank and terminated at the downstream end by an orifice discharging to the atmosphere A hydraulic siren, operating at a branch in the system immediately upstream of the discharge orifice, provides the oscillating hydraulic disturbance to the system during the dynamic tests The siren is capable of sweeping a continuous frequency range of 100–1000 cps when driven by a 5-hp, remotely controlled, d c variac motor

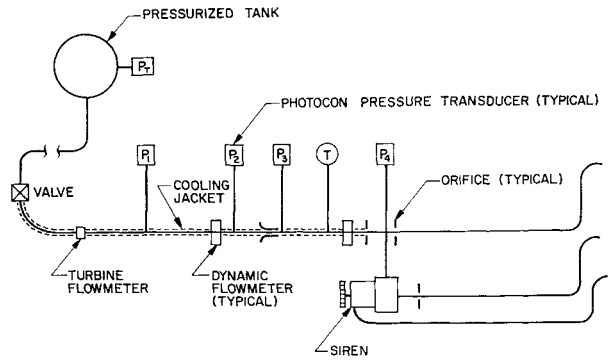

Fig 1 Test system configuration

Low pressure drop and effective fluid dynamic decoupling were desirable features for the intended venturi application According to Ref 5, the 7° diffuser included angle would insure a minimum pressure energy loss The venturi entrance contour was designed to have a radius, equal to twice the throat diameter, that would be conducive to efficient flow entry and at the same time leave more venturi length available for the diffuser The over-all length was limited by the space in the parent hardware

Instrumentation included Photocon pressure transducers to monitor the pressure oscillations, dynamic flowmeters (strain-gage, cantilever type) to record the oscillatory flow component, and Fastax camera recording equipment to determine the size and response of the cavitation bubble for variations in the pressure downstream of a lucite venturi A large electronic amplification is required to make the dynamic flow data measurable Amplification was accomplished *before* the flow signal was recorded on tape so that further amplification before playback was held to a minimum, thus limiting amplification of the tape noise

Test Procedure

With the system fluid flowing through the venturi under the prescribed tank pressure of 1500 psi, the siren was operated over the full frequency range of interest, 100–1000 cps, with all transducer outputs being recorded on tape for later analysis Only oscillatory components of the pressure and flow

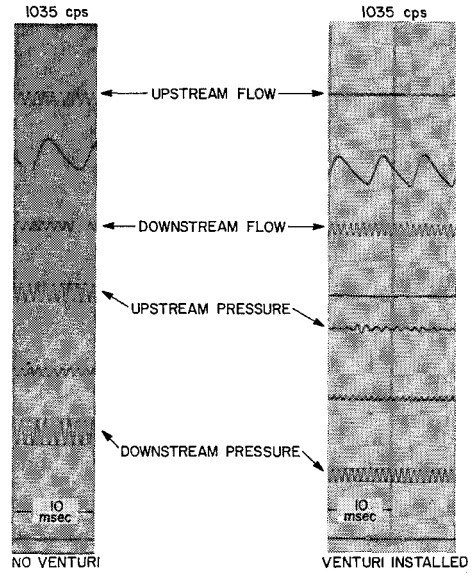

Fig 2 Typical filtered traces

Received September 3, 1963; revision received January 27, 1964

* Research Specialist, Liquid Rocket Engineering Department, Rocketdyne Division Member AIAA

† Supervisor, Liquid Rocket Engineering Department, Rocketdyne Division

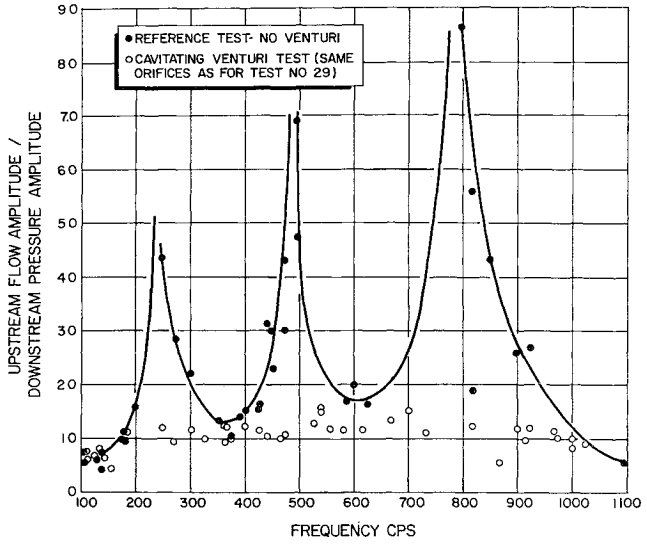

Fig 3 Frequency response for the $|\dot{w}_2|/|P_3|$ ratio

transducers were recorded to permit improved amplitude measurement accuracy This test was followed by an identical test, except for the replacement of the venturi by a cylinder of constant diameter (0 375 in), to provide reference data A comparison of the dynamic test data for the two tests was used as the basis for evaluating the effectiveness of the cavitating venturi in preventing the upstream transmission of flow os cillations that result from pressure oscillations generated downstream of the venturi

Liquid oxygen tests were conducted using essentially the same test sequence The chief difference was that these tests required a special precooling technique to insure that liquid, and not gaseous, oxygen was flowing in the system Before any testing commenced, liquid nitrogen was forced through the system jacket under low pressure (about 50 psi) for about 10 min to precool the test system Then liquid oxygen was allowed to flow through the test system under low pressure until liquid oxygen could be seen flowing out of the system discharges By this time, the thermocouple located downstream of the venturi indicated that the temperature had stabilized, and, according to Ref 6, this should have been ample precooling

Data Analysis

The results of the dynamic test data can be presented best as frequency response curves To be able to measure sine wave component amplitudes over the full-frequency range, the tape recorded data was played back through a variable band-pass filter onto oscillograph paper or Clevite brush recorder paper Narrow band passes were utilized to insure constant signal gain through the filter over the frequency band selected The traces of principal interest were the pressure oscillations generated downstream of the venturi and the pressure and flow oscillations transmitted upstream of the venturi For those particular filtered flow and pressure traces which displayed a very nearly sinusoidal wave shape within the same time slice, the ratio of flow amplitude measured immediately upstream of the venturi to pressure amplitude measured immediately downstream of the venturi was plotted vs frequency

Similar points were plotted for the traces obtained from both the venturi and reference tests A comparison of the resulting curves showed the effectiveness of the cavitating venturi in decoupling the downstream pressure oscillations from the upstream flow Figure 2 shows sample traces of the filtered data obtained with the test system transducers Amplitudes for frequency-response plots are measured from traces of this type

Test Results in Water

The lucite venturi, with a 0 160 in throat diameter and a 7° diffuser included angle, exhibited cavitation in water at a downstream pressure of 1100 psi (Upstream pressure was 1500 psi) For a brass venturi in water, with highly polished diffuser surface, the corresponding downstream pressure for incipient cavitation increased to 1325 psi In liquid oxygen, this pressure was 1350 psi Dropping the downstream pressure below the point of incipient cavitation, of course, insured deeper cavitation; however, the increased venturi pressure loss was undesirable The test points for the brass venturi were determined with the siren in the test system operating at 500 cps

Fastax motion picutres depict how the size of the cavitation bubble changes with a change in the pressure downstream of the venturi The bubble appears as a dark, wavy shadow emanating from the venturi throat When projected, the motion picture shows the cavitation bubble oscillating at the same constant frequency at which the siren was operating (1000 cps)

A frequency response curve shows the results of the dynamic tests The points in Fig 3 are a plot of the ratio of the upstream oscillating flow amplitude to the amplitude of the downstream oscillating pressure vs frequency It can be seen that resonances occur at approximately 250,500 and 800 cps With the constant diameter flow passage replaced by the cavitating venturi, the magnitudes of these resonances are significantly reduced, by a factor of approximately 5:1, as indicated by the small circles in the figure The flow to-pressure ratio holds some analogy to the ratio of the amplitude of an oscillating injector flow to the chamber pressure oscillation amplitude in a liquid rocket engine

Test Results in Liquid Oxygen

The test results in liquid oxygen paralled those obtained in water, showing a 5:1 reduction in upstream pressure amplitudes in the vicinity of the resonances Steady flow tests showed that incipient cavitation in the identical venturi occurred at a slightly higher pressure downstream of the venturi, 1350 psi compared to 1325 psi for water

Conclusions

From these results it can be concluded that a cavitating venturi flowing water or liquid oxygen is significantly effective in decoupling downstream pressure oscillations from the upstream flow over a frequency range of 100–1000 cps Downstream pressure oscillations of large amplitude (greater than 100 psi peak to-peak) could extend partially into the noncavitating region and make the venturi less effective while it is operating at the point of incipient cavitation Erosion due to cavitation was not apparent in the brass venturi

The cavitation bubble has some appearances of behaving as a hydraulic capacitor, releasing some of the pressure energy of the oscillations as they are propagated upstream through the central core[7] of the bubble Fastax movies demonstrated the good frequency response of the cavitation bubble in water, oscillating at a frequency of 1000 cps as it adjusted in size to the downstream pressure variation of the same frequency

References

[1] Dodge, R A and Thompson, M J , *Fluid Mechanics* (Mc Graw-Hill Book Co , Inc , New York, 1937), 1st ed , Chap V, pp 100–106

[2] Fox, Z , "Cavitating venturi for small pulsing rockets," Space Aeronaut **39**, 141–145 (1962)

[3] Sverdrup, N M , "Theory of hydraulic flow control," Prod Eng **26**, 161–176 (1955)

[4] Rouse, H , *Fluid Mechanics for Hydraulic Engineers* (McGraw-Hill Book Co , Inc , New York, 1938), 1st ed Chap VI, pp 129–135

[5] Streeter, V L, *Fluid Mechanics* (McGraw-Hill Book Co, Inc, New York, 1951), 1st ed, Chap VII, p 215
[6] Shufflebotham, N, 'A method of detecting the fully cooled state of a liquid oxygen pipeline," Rocket Propulsion Establishment, Westcott, England, Tech Memo 196, p 5 (1959)
[7] Randall, L N, "Rocket applications of the cavitating venturi," ARS J **22**, 28–31 (1952)

Skin Friction of Slender Cones in Hypersonic Flow

JAN RAAT*
U S Naval Ordnance Laboratory, White Oak, Silver Spring, Md

The transverse-curvature effect on the skin friction of slender, circular cones is investigated employing a momentum-integral technique A relation between a suitable transverse-curvature parameter and the hypersonic viscous interaction parameter is discussed

1 Introduction

APPLICATION of the Mangler transformation reduces the axisymmetric boundary-layer problem to the computation of a two-dimensional boundary layer The transformation becomes possible through the assumption that the radial coordinate, wherever it occurs explicitly in the boundary-layer equations, may be replaced by the local body radius In other words, it is assumed that the body radius is large compared with the boundary-layer thickness This assumption may become invalid, however, for slender bodies in hypersonic flight at high altitudes, such as the case of reentry missiles It will then be necessary to solve the boundary-layer equations with the additional transverse-curvature terms Unfortunately, these equations, in general, do not yield similar solutions In the regime of vanishing transverse-curvature effects, however, asymptotic solutions have been obtained by Probstein and Elliott [1] In the following, a momentum-integral technique is discussed which has been employed to obtain an approximate solution in the regime where transverse-curvature effects are neither very small nor very large, and where, consequently, series-expansion techniques fail

2 Analysis

In the absence of pressure variations the momentum loss in the boundary layer is due to friction only, and the momentum theorem requires

$$\frac{d}{dx}\int_0^\infty \rho u(u - u)2\pi r dy = 2\pi r_w \tau_w \tag{1}$$

where conventional notation has been adopted †

Introduction of the variable

$$\lambda = \int_0^y \frac{\rho}{\rho} r dy$$

reduces Eq (1) to the incompressible form

$$\frac{d}{dx}\int_0^\infty \frac{u}{u_e}\left(1 - \frac{u}{u_e}\right) d\lambda = \frac{r_w \tau_w}{\rho u^2} \tag{2}$$

It can be shown[2] from the governing boundary-layer differential equations that, for a heat-insulating wall and for a gas following the Chapman-Rubesin viscosity law $\mu/\mu = C\,T/T$, the velocity profile $u/u = f(x,\lambda)$ can be expressed as

$$f(x,\lambda) = \frac{1}{\Phi}\frac{\partial f(x,0)}{\partial \lambda}\left[\Phi\lambda - \frac{1}{2}\Phi^2\lambda^2 + \frac{1}{3}\Phi^3\lambda^3 + O(\lambda^4)\right]$$

where

$$\Phi = \frac{2\cos\theta}{r_w^2}\frac{T_w}{T}$$

The angle θ is the local inclination of the body surface with respect to the freestream (in the case of a cone, θ is the semivertex angle)

The foregoing expansion indicates that a profile proportional to $\ln(1 + \Phi\lambda)$ will give a fairly accurate estimate of the actual boundary-layer flow near the body surface, because such a profile will be correct up to the fourth order in $\Phi\lambda$ It further can be shown that, for a gas following a power viscosity law instead of the linear Chapman-Rubesin relation, the logarithmic profile is correct up to only the third order in $\Phi\lambda$ This will also be the case for a heat-conducting surface If we choose the profile‡

$$f(x,\lambda) = [1/\alpha(x)]\ln(1 + \Phi\lambda)$$
$$f(x,\lambda) = 1 \text{ for } \lambda \geq (1/\Phi)(e^\alpha - 1) \tag{3}$$

the following differential equation for $\alpha(x)$ is obtained upon introducing Eq (3) into Eq (2):

$$\frac{d}{dx}\left[\frac{r_w^2}{\cos\theta}\left\{\frac{2}{\alpha^2}(1 - e^\alpha) + \frac{1}{\alpha}(1 + e^\alpha)\right\}\right] = \frac{4\mu_w \cos\theta}{\rho_w u_e \alpha} \tag{4}$$

Equation (4) is still applicable to a body of revolution of arbitrary shape as long as pressure variations along the body are negligible Integration of Eq (4) in the particular case of a cone leads to the following expression for the local skin-friction coefficient[2]:

$$C_f = \frac{\tau_w}{\frac{1}{2}\rho_e u^2} = [1 + F(t)]\left(\frac{C\nu_e}{u\,x}\right)^{1/2} \tag{5}$$

where

$$t = \cot\theta\,\frac{T_w}{T}\left(\frac{C\nu}{u\,x}\right)^{1/2} \tag{6}$$

The parameter t is the transverse-curvature parameter of Probstein and Elliott, multiplied by $3^{1/2}T_w/T$ The functional dependence $F(t)$ has been computed from the numerical solution for α and is given in Fig 1 Furthermore, the following asymptotic solutions for $F(t)$ can be derived from Eq (4):

$$F(t \to 0) = \tfrac{4}{5}t - \tfrac{1}{25}t^2 + \tag{7}$$

$$1 + F(t \to \infty) = 4t[\ln^{-1}(4t^2) - \ln^{-3}(4t^2) + (-\tfrac{7}{2})\ln^{-4}(4t^2) + \quad] \tag{8}$$

Equation (7) applies to the regime of vanishing curvature effects far downstream of the cone apex, whereas Eq (8) applies to the immediate vicinity of the cone apex in the regime of very strong curvature effects

Received December 27, 1963 This work was performed in connection with research sponsored by the Bureau of Naval Weapons, Department of the Navy

* Aerospace Engineer

† The coordinates x and y, respectively, are parallel and normal to the body surface with the origin at the body apex or leading edge; r is the radial coordinate The subscripts e and w, respectively, refer to the outer edge of the boundary layer and the body surface

‡ For incompressible flow and $\theta = 0$, Eq (3) reduces to the profile employed by Glauert and Lighthill[3] in their analysis of the boundary layer along a slender, circular cylinder